Spectroscopy and Photophysics of Indoline and Indoline-2-Carboxylic Acid

Michael W. Allen, Jay R. Unruh, Brian D. Slaughter, Sarah J. Pyszczynski, Thaddaus R. Hellwig, Tim J. Kamerzell, and Carey K. Johnson*

University of Kansas, Department of Chemistry, 1251 Wescoe Hall Drive, Lawrence, Kansas 66045

Received: December 23, 2002; In Final Form: May 6, 2003

This paper presents a detailed description of the fluorescence and photophysical behavior of indoline and indoline-2-carboxylic acid (I2CA). Indoline is an analogue of indole lacking the $C_2{=}C_3$ double bond, but unlike indole, indoline possesses well-separated ^1L_a and ^1L_b states. I2CA, which displays similar fluorescence properties, is an amino acid and can be regarded as a fluorescent analogue of proline. In view of the potential for indoline and I2CA as fluorescent probes in peptides and proteins, we have undertaken an in-depth study of the spectroscopic and photophysical properties of these molecules. A companion paper (Slaughter, B.D.; Allen, M. W.; Lushington, G. H.; Johnson, C. K. *J. Phys. Chem. A* **2003**, *107*, 5670) presents a theoretical treatment of the spectroscopic transitions of indoline and I2CA. The pH-dependent absorption and fluorescence characteristics are investigated for both indoline and I2CA. Ground- and excited-state dissociation constants are determined spectroscopically. Quantum yields and radiative lifetimes are reported, and relaxation mechanisms are explored for both indoline and I2CA. Comparisons are made to the model systems of aniline and indole. The fluorescence lifetime of indoline is 4 to 7 ns in nonaqueous solvents but is reduced to 0.18 ns in water by electron-transfer quenching. The fluorescence decays of I2CA indicate the presence of two conformations, one with a short (<1 ns) lifetime and the other with a lifetime of 4 to 5 ns in most solvents. The fluorescence properties of I2CA in water are unvaried from pH 6−10 with a fluorescence decay component of 5.0 ns that makes it useful as a potential fluorescence probe.

Introduction

The environmental sensitivity of the fluorescence of the amino acid tryptophan and derivatives of its side chain, indole, is often exploited to examine peptides and proteins.[1−4] The intrinsic environmental sensitivity of indole results from competing relaxation pathways that have been the object of many studies.[5−9] Suggested mechanisms for nonradiative decay in aromatic amines such as tryptophan include photoionization,[10] intersystem crossing,[11] and proton-[12,13] and electron-transfer reactions.[14,15] The existence of multiple rotomers,[6,8,16−19] each with different decay rates, and the close proximity of the ^1L_a and ^1L_b absorption bands[20−23] complicate the relaxation pathways in tryptophan. Changes in solvent polarity,[24] temperature,[7,15] and pH[7] can greatly affect the fate of the excited state of indole and related compounds.

In this paper, we focus on the photophysical properties of indoline and indoline-2-carboxylic acid (I2CA), compounds that differ from indole and indole-2-carboxylic acid by the lack of a double bond in the five-membered ring (Figure 1). In a companion paper,[25] we describe theoretical calculations of the electronic states and the ground- and excited-state properties of indoline and I2CA. We have recently shown that I2CA can be incorporated into short peptides as a fluorescent probe of the reorientational dynamics of the peptide backbone.[26−28] Given the complexity of the fluorescence decay of indole itself, and to an even greater extent of tryptophan, it is important that the photophysics of indoline be thoroughly examined. I2CA, which can be regarded as a product of the fusion of a benzene ring to carbons 4 and 5 of proline, is a fluorescent analogue of proline.

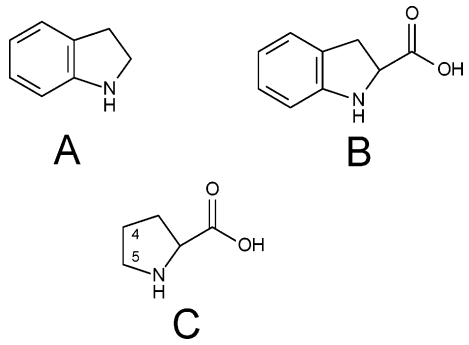

Figure 1. Structures of (A) indoline, (B) indoline-2-carboxylic acid, and (C) proline.

The (*S*)-(−)-indoline-2-carboxylic acid isomer retains the same stereochemistry as the L-amino acids. We have recently shown through the calculation of energy-minimized structures that I2CA nearly identically preserves the structural properties of proline.[28,29] The substitution of indoline for proline rigidly links the emission dipole moment of the fluorophore to the backbone motion of the peptide and eliminates contributions from the independent motions of a fluorescent side chain attached to the peptide backbone by a single C−C bond. This allows for the direct fluorescence examination of peptide backbone motions.

The present paper undertakes a detailed investigation of the photophysics of indoline and I2CA. The fluorescence properties of indoline and I2CA are examined using the spectroscopic properties of aniline as a model. Spectroscopic titration of indoline and I2CA reveals dissociation constants for the amine group of indoline and the amine and carboxylic acid groups of

* Corresponding author. E-mail: ckjohnson@ku.edu.

10.1021/jp027813p CCC: $25.00
Published on Web 07/02/2003

I2CA. Absorption and emission spectra are used to determine excited-state dissociation constants (pK_a^*) for indoline and I2CA. Both the radiative lifetime and the fluorescence lifetime of indoline and I2CA are determined under various solvent conditions and used to elucidate the quenching mechanisms of indoline and I2CA. The fluorescence quantum yield of indoline and I2CA is calculated from the radiative lifetime and determined by direct comparison to amino acids with a known quantum yield.

Methods and Materials

Chemicals. The highest purity aniline (99%), indoline (99%), and indoline-2-carboxylic acid (97%) were all obtained from the Aldrich chemical company (St. Louis, MO). Indoline and I2CA were used as received. Aniline was dried over KOH, purified by a single vacuum distillation, and diluted immediately with the appropriate solvent. Acetonitrile, cyclohexane, dimethyl sulfoxide, ethanol, hydrochloric acid, methanol, sulfuric acid, tetrahydrofuran, triethylamine, and trifluoroethanol were all obtained from Fisher Scientific in the highest purity possible. All solvents were used without further purification.

For the spectroscopic titration experiments, the appropriate 50 mM phosphate buffer (Fisher) was diluted to 5 mM, the analyte was dissolved, the pH was adjusted with dilute HCl and NaOH solution, and the solution was filtered using 200-nm syringe filters (Arcodisk, Pall Corporation). For all other aqueous solutions, indoline and I2CA were dissolved in type I reagent-grade water (Barnstead model D4641), and the pH was adjusted with dilute HCl and NaOH solutions. All solutions were purged with a slow stream of nitrogen gas for a minimum of 10 min prior to fluorescence analysis.

Absorption and Emission Spectra. Absorption spectra were measured on either a Varian Bio 50 or a Varian Bio 100 UV/visible spectrophotometer. A blank absorption spectrum was acquired for each solvent. To minimize variations, the same quartz cuvette (NSG Precision Cells, Inc.) was used to collect the background and absorption spectra. Background-corrected spectra were then used for subsequent analysis and calculations. Solutions of precisely known concentration were used to determine the extinction coefficients for aniline, indoline, and I2CA. Absorption spectra for the spectroscopic titration and radiative lifetime determinations were collected using aniline, indoline, and I2CA concentrations of 50 μM or less under all solvent conditions. For the quantum yield experiments, the optical density of all solutions was kept below 0.05 at the lowest-energy absorption maximum to minimize inner filter effects.

Fluorescence emission spectra were collected on a Quantamaster Fluorimeter (Photon Technologies International) with an instrumental bandwidth of 5 nm or less. Fluorescence spectra for the spectroscopic titration and radiative lifetime experiments were acquired with the same solutions used for absorption experiments. A background emission scan was obtained for each solvent and used to subtract Raman scattering and intense arc lamp lines. Only background-subtracted spectra were used for subsequent analysis and calculations.

Time-Correlated Single-Photon Counting. Fluorescence lifetimes were determined by time-correlated single-photon counting (TCSPC) with an instrument described previously.[30] Lifetimes were determined from fluorescence emission collected at the magic angle to eliminate rotational contributions. Under all solvent conditions, the concentration of aniline, indoline, and I2CA solutions was 50 μM or less. Aniline solutions were excited at 287 nm, and the fluorescence emission was collected at 322 nm. All indoline and I2CA solutions were excited at 305 nm by the frequency-doubled output of a synchronously pumped dye laser, and the fluorescence emission collected at 355 nm was discriminated by a monochromator (American Holographics DB-10) with a 10-nm bandwidth. Fluorescence lifetime decays were globally fit with the nonlinear least-squares algorithm of the Globals Unlimited software package.[31] Fluorescence lifetimes were determined from the global fit of a minimum of four decay measurements for each sample. For fits with multiple decay components, the amplitude of each component was allowed to vary over each of the individual fluorescence decays and was later normalized. Goodness of fit was evaluated from χ^2 plots and a visual inspection of the residuals. Uncertainties were estimated by *F*-test confidence interval analysis to find the range of values of the fitting parameter that increase χ^2 within a confidence limit of one standard deviation while all other fitting parameters are freely varied.

Ground-State Dissociation Constants. For the spectroscopic titration experiments using absorption spectra, the dissociation constant for a single ionization was determined by fitting the measured extinction coefficients to a form of the Henderson−Hasselbalch equation

$$\epsilon = \frac{\epsilon_{HA} + 10^{(pH - pK_a)}\epsilon_{A^-}}{1 + 10^{(pH - pK_a)}} \quad (1)$$

where ϵ is the measured extinction coefficient and $\epsilon_{HA}$and ϵ_{A^-} are the extinction coefficients of the protonated and deprotonated species, respectively. A similar equation can be employed to determine dissociation constants when the protonated and deprotonated species have different fluorescence emission intensities. For the absorption spectroscopic titration of a diprotic equilibrium, the following equation was employed:

$$\epsilon = \frac{10^{-pH}\epsilon_{H_2A^+} + 10^{-pK_{a1}}\epsilon_{HA} + 10^{(pH - pK_{a1} - pK_{a2})}\epsilon_{A^-}}{10^{-pH} + 10^{-pK_{a1}} + 10^{(pH - pK_{a1} - pK_{a2})}} \quad (2)$$

The extinction coefficients of acidic, intermediate, and basic species are represented by $\epsilon_{H_2A^+}$, ϵ_{HA}, and ϵ_{A^-} , respectively. The equilibrium constant for the loss of the first proton is given by pK_{a1}; likewise, pK_{a2} is the equilibrium constant between the intermediate and basic forms.

Decay-Associated Spectra. Fluorescence decays were collected for I2CA in 10-nm increments between 320 and 400 nm. When the decay constants of a multiple-component decay do not change with wavelength, the decay-associated spectra (DAS) can be calculated for each decay component. The DAS are given by[31]

$$I_i(\lambda) = \frac{\alpha_i(\lambda)\,\tau_i F(\lambda)}{\sum_j \alpha_j(\lambda)\,\tau_i} \quad (3)$$

where $\alpha_i(\lambda)$ is the wavelength-dependent amplitude, τ_i is the wavelength-independent lifetime of component *i*, and $F(\lambda)$ is the steady-state fluorescence intensity.

Quantum Yield. The quantum yields for indoline and I2CA were determined by two methods. In the first method, the quantum yield was determined relative to a reference compound of known quantum yield. The integrated fluorescence intensity of the analyte (*I*) and reference (I_R), the optical density of the analyte (*OD*) and reference (OD_R), and the refractive index of

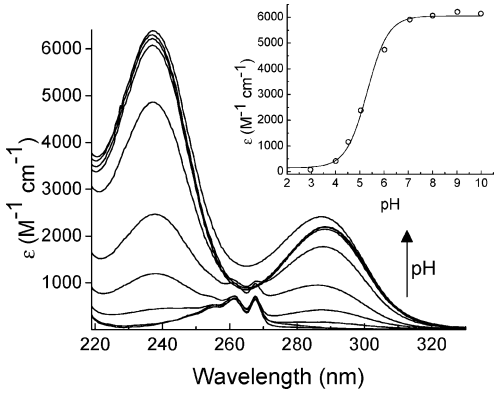

Figure 2. Absorption spectrum of indoline in phosphate-buffered solutions from pH 2 to 10. Inset: Spectroscopic titration of the ^1L_a absorption band at 238 nm. The solid line is the fit to the Henderson−Hasselbalch equation.

the analyte (n) and reference (n_R) are related to the quantum yield of the analyte according to[32]

$$Q = Q_R \frac{I}{I_R} \frac{OD_R}{OD} \frac{n^2}{n_R^2} \tag{4}$$

where Q_R is the quantum yield of the reference compound. Tyrosine and tryptophan were used as references, and their aqueous quantum yields were taken to be 0.07[30] and 0.14,[33] respectively.

The second method used to determine the quantum yield employed the method of Strickler and Berg[34] as modified by Birks and Dyson[35] to calculate the radiative lifetime (τ_0). The quantum yield (Q) was determined from

$$Q = \frac{\tau_f}{\tau_0} \tag{5}$$

where τ_f is the fluorescence lifetime. The radiative lifetime was calculated from the integrated absorption and emission spectra by the equation

$$\frac{1}{\tau_0} = 2.880 \times 10^{-9} \frac{n_f^3}{n_a} \langle \omega_f^{-3} \rangle_{av}^{-1} \int \epsilon(\omega)\, \mathrm{d} \ln \omega \tag{6}$$

where n_f and n_a are the refractive indices of the solution at the emission and absorption wavelengths,[36] ω is the wavenumber of absorption, ω_f is the emission wavenumber, and $\epsilon(\omega)$ is the absorption extinction coefficient. The integral was evaluated by fitting absorption spectra to a sum of four or five Gaussians. The average $\langle \omega_f^{-3} \rangle_{av}^{-1}$ was obtained from

$$\langle \omega_f^{-3} \rangle_{av}^{-1} = \frac{\int I(\omega)\, \mathrm{d}\omega}{\int \omega^{-3} I(\omega)\, \mathrm{d}\omega} \tag{7}$$

Results and Discussion

Absorption and Fluorescence Spectra and Titrations: Indoline Absorption and Fluorescence Spectra. Absorption spectra of indoline in 5 mM phosphate buffers of varying pH are shown in Figure 2. Distinct features of the indoline absorption spectrum at low and high pH define two pH regimes. In the low pH regime (pH 2−5), weak bands are present at 261 and 267 nm. As pH is increased, the bands at 261 and 267 nm weaken until vanishing near neutral pH as new absorption bands grow in, centered at 287 and 237 nm. In this respect, indoline is nearly identical in its pH-dependent absorption behavior to aniline. These absorption bands, in the high pH regime, are assigned to the ^1L_b and ^1L_a states, respectively.[25]

Aniline in the low pH regime shows two low-energy absorption bands at 260 and 254 nm. In the high pH regime, aniline exhibits two broad absorption features centered at 280 and 230 nm corresponding to ^1L_b and ^1L_a states.[37,38] For both aniline and indoline, the increased absorption strength and longer absorption wavelength in the high pH regime can be attributed to resonance structures extending conjugation to the nitrogen atom. In the low pH regime, the hybridization of the protonated nitrogen ($>NH_2^+$) eliminates contributions from these resonance structures. This point is discussed in greater detail in the companion paper.[25]

A comparison of the indoline and aniline absorption and emission data is found in Table 1. The intensity of the ^1L_a absorption band of aqueous indoline solutions from 5 to 500 μM increased linearly as described by the Beer−Lambert law. This linear relationship of concentration and absorption indicates that aggregation is not occurring in this concentration range, which exceeds the range of concentrations of solution examined.

The fluorescence emission spectrum of indoline is shown in Figure 3. Indoline fluorescence increases in intensity and decreases in energy with increasing pH. In the low pH regime, the wavelength of maximum fluorescence emission is 337 nm. As the pH increases, the fluorescence spectrum red shifts to 364 nm. Maximum fluorescence intensity is achieved in the high pH regime. Like indoline, the fluorescence of aniline varies in intensity as a function of pH. However, unlike indoline, the fluorescence emission band does not shift to lower energy with increasing pH.[39]

The fluorescence emission spectra of indoline in cyclohexane, acetonitrile, ethanol, and water are shown in Figure 4. The fluorescence emission shifts to longer wavelengths as the solvent polarity (as measured by the $E_T(30)$ parameter, for example) increases. This polarity dependence indicates an increase in the dipole moment in the fluorescing L_b state relative to the ground state. An increase in the dipole moment in both L_a and L_b excited states has been confirmed by ab initio calculations as described in the companion paper.[25]

Indoline Titration. The change in protonation state of the amine functionality of indoline from a cationic (NH_2^+) to a neutral (NH) form elicits a change in the intensity and frequency of the ^1L_a and ^1L_b absorption bands. The change in intensity of the ^1L_a band of indoline was used to determine the ground-state dissociation constant (pK_a) by spectroscopic titration. The ground-state pK_a can also be obtained from the red-shifting peak maximum of indoline fluorescence emission. The spectroscopic titrations of the ^1L_a (inset of Figure 2) and ^1L_b (data not shown) absorption bands of indoline yield pK_a values for the amine functionality of 5.3 ± 0.04 and 5.2 ± 0.06, respectively, when fit to the Henderson−Hasselbalch equation (eq 1). Similarly, a fit of the wavelength of maximum fluorescence plotted as a function of pH (inset of Figure 3) yields a pK_a of 4.6 ± 0.03. The apparent decrease in the pK_a measured from the fluorescence emission may reflect the decrease in the pK_a of indoline in the excited state (vide infra). Deprotonation of the amine in the excited state may occur on a time scale comparable to the fluorescence lifetime. In that case, the emission spectrum at pH values below the ground-state pK_a but well above the excited-state pK_a may contain contributions from the basic form. However, because equilibrium between the cationic and neutral

TABLE 1: Absorption and Fluorescence Properties of Aniline, Indoline, and I2CA

	solvent	λ_{max} abs (nm)	f [a]	λ_{max} fluorescence (nm)	Stokes shift (cm^{-1})	$\langle\tau_f\rangle$ (ns)[b]	Φ[c] calculated	Φ[d] measured	Φ[e] measured
aniline	water pH 7	280	0.16 (^1L_a) 0.03 (^1L_b)	337	6040	3.9[f]	0.024	0.012	0.015
	acetonitrile	287		322	3790	3.0 ± 0.013	0.052	0.044	0.068
indoline	water pH 7	288	0.16 (^1L_a) 0.05 (^1L_b)	362	7100	0.18 ± 0.004	0.005	0.006	0.007
	acetonitrile	300		353	5000	4.30 ± 0.012	0.157	0.090	0.083
I2CA	water pH 7	286	0.16 (^1L_a) 0.06 (^1L_b)	354	6720	1.26 ± 0.020	0.069	0.127	0.110
	acetonitrile	292		351	5760	0.79 ± 0.015	0.037	0.030	0.026

[a] Calculated following ref 56. [b] Average of fluorescence lifetime components weighted by their amplitudes. [c] Calculated from eq 5 (see text). [d] Quantum yield measured relative to that of tyrosine. [e] Quantum yield measured relative to that of tryptophan. [f] From ref 58.

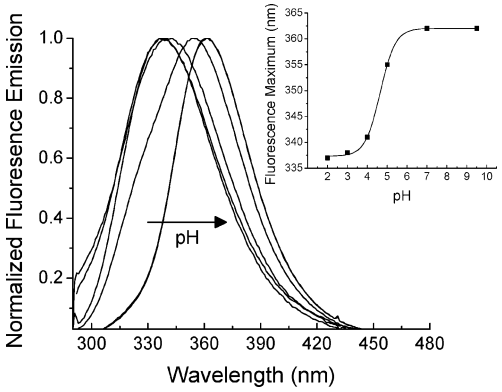

Figure 3. Fluorescence emission spectra of indoline in phosphate-buffered solutions from pH 2 to 10. Inset: Spectroscopic titration curve of the wavelength of maximum fluorescence intensity. The solid line is the fit to the Henderson−Hasselbalch equation.

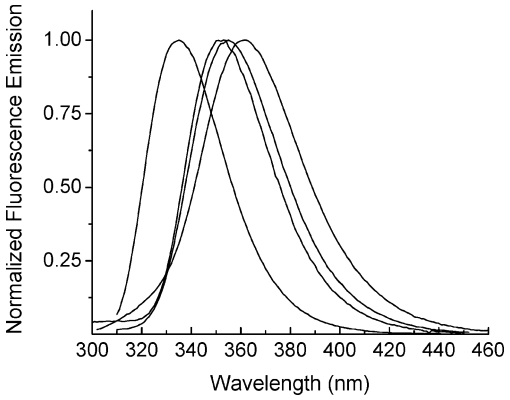

Figure 4. Fluorescence emission of indoline in various solvents. The peaks shift to the red in the following order: cyclohexane, acetonitrile, ethanol, and water (pH 7).

forms is not reached within the fluorescence lifetime of indoline, the pK_a determined from the fluorescence data does not correspond to the value calculated for the excited state.

The spectroscopic pK_a determined for indoline corresponds closely to results for aniline. A fluorescence intensity titration has determined a value of 4.5 for the ground-state pK_a of aniline.[39] This value is in good agreement with conventional titrations of aniline that yielded a pK_a of 4.58.[40] The higher ground-state pK_a determined for indoline is reasonable for a secondary amine. The inductive effect of alkyl-chain addition to the nitrogen increases the pK_a to 4.85 for *N*-methylaniline and 5.11 for *N*-ethylaniline.[41]

Indoline-2-Carboxylic Acid Absorption and Emission Spectra. Absorption spectra of I2CA in 5 mM phosphate buffers

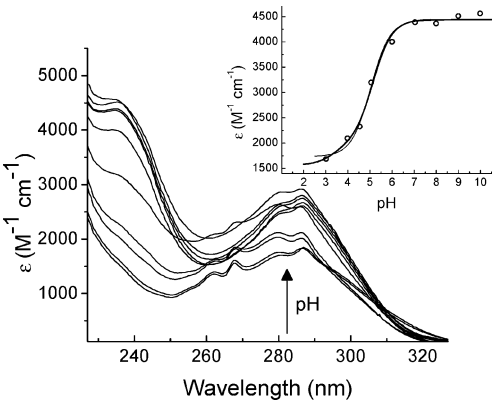

Figure 5. Absorption spectrum of I2CA in phosphate-buffered solutions from pH 2 to 10. Inset: Spectroscopic titration curve of the ^1L_a absorption band. Light and bold lines are the fits to a mono- and diprotic equilibrium, respectively.

of varying pH are shown in Figure 5. The lowest-energy absorption band (^1L_b) of I2CA is broad and centered around 285 nm. As it does for indoline, the extinction coefficient of the ^1L_b absorption band of I2CA increases with increasing pH. However, unlike that of indoline, the ^1L_b band of I2CA is intense in both the high- and low pH regimes. Overall, the ^1L_b band of I2CA is broader and more intense than the ^1L_b absorption band of indoline. At low pH, the long-wavelength band decreases in intensity but does not disappear, in contrast to the corresponding spectra of indoline (Figure 2). Broadening also becomes apparent on the low-energy side of the band as the pH decreases below pH 4. Two weak absorption features are present in the I2CA absorption spectrum at 268 and 262 nm below pH 5. These bands are similar to features found in the low pH regime absorption spectra of aniline and indoline (Figures 2 and 3). As in aniline and indoline, these bands may represent transitions centered on the phenyl ring with little contribution from the five-membered ring. The ^1L_a absorption band of I2CA, centered at 237 nm, is less intense than the ^1L_a band of indoline. The intensity of the band is low under acidic conditions but develops as the pH is increased.

As shown in Table 1, the oscillator strength of the ^1L_b absorption band is nearly a factor of 2 times larger for indoline compared to that for aniline and a factor of 1.2 times greater for I2CA compared to that for indoline. At neutral pH, the ratio of the oscillator strength of ^1L_a and ^1L_b absorption bands in aniline is 5.3; this ratio drops to 3.2 for indoline and to 2.7 for I2CA. This trend indicates mixing of the ^1L_a and ^1L_b states, leading to mixed spectroscopic properties. Mixing of ^1L_a and ^1L_b states has also been observed in quantum calculations of these compounds.[25]

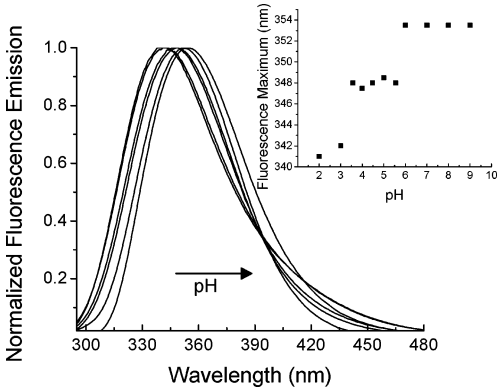

Figure 6. Fluorescence emission of I2CA in phosphate buffered solutions from pH 2 to 10. Inset: Spectroscopic titration curve of the wavelength of maximum fluorescence intensity.

The absorption spectrum of I2CA (Figure 5) reveals cationic, zwitterionic, and anionic states. The two lowest pH solutions (2 and 3) reveal a feature shifted to the red in the ^1L_b band that is absent in higher pH solutions. This absorption feature results from the cationic form of I2CA, where a net positive charge results from the protonated amine and carboxyl groups. This red-shifted absorption feature vanishes at pH values above 3. At still higher pH values, the two weak absorption bands at 262 and 268 nm vanish while the intensity of the 285-nm band increases. The observation of changes in the absorption spectrum in two distinct steps with increases in pH demonstrates the influence of distinct deprotonation steps as the pH is increased. The long-wavelength feature below pH 3 can be assigned to the protonation of the carboxylic acid. This long-wavelength feature disappears above the pK_a of the carboxylic acid, yielding the absorption spectrum of the zwitterionic state. By analogy with indoline, the loss of two weak absorption bands at 262 and 268 nm can be assigned to the deprotonation of the amine in I2CA. These features are analogous to absorption features present in aniline and indoline (Figure 2) and are used to distinguish cationic and neutral states in those two molecules. Above neutral pH, these two absorption features vanish, resulting in the absorption spectrum of the anionic state of I2CA.

As Figure 6 illustrates, the fluorescence emission spectrum of I2CA red shifts with increasing pH. At pH 2, where I2CA is in a cationic state, the wavelength of the fluorescence maximum of I2CA is 341 nm. In the zwitterionic state, around pH 5, the peak shifts to 349 nm. In the anionic sate, at neutral pH and above, the fluorescence maximum shifts to 354 nm. This red shift of the fluorescence spectrum with pH gives clear spectroscopic evidence for the cationic, zwitterionic, and anionic forms of I2CA in solution. The inset of Figure 6 clearly shows the three states of I2CA represented by the red-shifting maximum of fluorescence emission.

The fluorescence maxima of I2CA in DMSO, acetonitrile, and methanol shift to longer emission wavelength with higher polarity (Figure 7). I2CA in water does not follow this pattern. The emission maximum of I2CA in water is similar to that in DMSO and acetonitrile (both of which are much less polar solvents) but with a much broader emission band. The blue-shifted emission suggests that the I2CA ground state is hydrogen bonded in water. The width of the emission band in water suggests a range of hydrogen-bonded structures.

Indoline-2-Carboxylic Acid Titration. The inset of Figure 5 shows the spectroscopic titration of the L_a absorption band (235 nm) of I2CA. When this titration is fit to a Henderson−Hasselbalch equation for a single proton dissociation (eq 1), a ground-state pK_a of 5.0 is obtained. However, as discussed

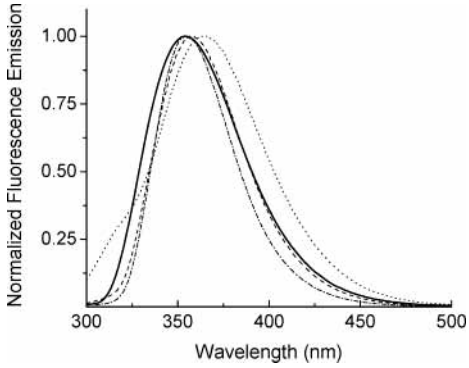

Figure 7. Fluorescence emission of I2CA in water (—), DMSO (— · —), acetonitrile (— —), and methanol (··)

above, the absorption spectra of I2CA indicate the effect of two pH-dependent equilibria. An improved fit (as judged by χ^2) of the ^1L_a absorption band titration curve is obtained for a fit to a diprotic equilibrium (eq 2). The first ionization constant is assigned to the carboxylic acid functionality. The value determined for the first ionization constant of I2CA of 3.3 is in good agreement with the pK_a of the carboxylic acid functionality of proline, 2.9. The second pK_a obtained for I2CA of 5.1 corresponds to the dissociation of the amine proton, as in aniline and indoline.

Evidence for the cationic, zwitterionic, and anionic states of I2CA is also found in the fluorescence emission spectrum (Figure 6). The isoemissive point at 397 nm results from the fluorescence emission shift of the cationic form relative to the zwitterionic form of I2CA. Because this emission feature is present only in the pH 2 and 3 solutions, it must represent the fluorescence of the cationic state. The red shift of the wavelength of maximum fluorescence intensity as a function of pH is shown in the inset of Figure 6. The large red shifts between pH 3 and 3.5 and between pH 5.5 and 6.0 are indicative of the dissociation of the carboxylic and amine protons, respectively.

Excited-State pK_a. The excited-state pK_a (pK_a^*) can be estimated from the change in the wavelength of maximum absorption for the cationic and neutral forms of indoline and the cationic, zwitterionic, and anionic forms of I2CA. According to the Förster cycle method,[42,43] the change in pK_a from the ground to the excited state is given by[44]

$$\mathrm{p}K_a^* - \mathrm{p}K_a = \left(\frac{10^7 hc}{2.303kT}\right)\left(\frac{\lambda_{A^-} - \lambda_{HA}}{\lambda_{HA}\lambda_{A^-}}\right)_a \qquad (8)$$

where the wavelength of maximum fluorescence or absorption of the protonated species is represented by λ_{HA} and the wavelength of maximum fluorescence or absorption of the deprotonated species is represented by λ_{A^-}.

The results of the pK_a^* calculations are found in Table 2. Estimations of pK_a^* from the absorption spectra of indoline and I2CA both show a dramatic increase in the acidity of the amine in the excited state. This is consistent with a negative excited-state pK_a generally found for aromatic amines[45] and is in good agreement with previously reported Förster cycle values of the pK_a^* reported for aniline.[39] In contrast, the excited-state pK_a of the carboxylic acid moiety of I2CA increases in the excited state. This trend is consistent with aromatic carboxylic acids, which generally have a more basic excited state.[46,47]

Table 2 also tabulates the estimated values of pK_a^* from the change in the wavelength of maximum fluorescence for each protonation state of indoline and 12CA. Although values calculated from the emission spectra agree with the trend

TABLE 2: Ground and Excited-State Dissociation Constants for Aniline, Indoline, and I2CA

	functional group	pK_a from ^1L_b absorption band	pK_a from ^1L_a absorption band	pK_a from λ_{max} of fluorescence	pK_a* from absorption	pK_a* from fluorescence
aniline	amine			4.5[a]		−0.50[a]
indoline	amine	5.2 ± 0.06	5.3 ± 0.04	4.6 ± 0.03	−0.59[b]	0.44[c]
12CA	carboxylic acid		3.3 ± 0.49[d]	3.0 ± 0.34	5.80[e]	4.42[c]
	amine	4.7 ± 0.12	5.1 ± 0.06[d] 5.0 ± 0.05[f]	5.7 ± 0.37	−0.57[b]	4.93[c]

[a] Value from ref 39. [b] Value determined from the ^1L_b absorption band using the method in ref 44. [c] Value determined using the pK_a obtained from the λ_{max} of fluorescence experiments. [d] Value from the diprotic fit of the absorption spectrum. [e] Value calculated by subtraction of the pH 5 from pH 2 absorption spectrum to obtain the absorbance of the cationic species. [f] Value from the Henderson−Hasselbalch fit.

TABLE 3: Fluorescence Lifetimes of Aniline, Indoline, and I2CA in Various Solvents

	aniline		indoline		I2CA					
solvent	τ_1 (ns)	χ^2	τ_1 (ns)	χ^2	τ_1 (ns)	a_1	τ_2 (ns)	a_2	χ^2	$\langle\tau_f\rangle$ (ns)
acetonitrile	2.90 ± 0.009	1.13	4.30 ± 0.012	1.47	0.16 ± 0.006	0.83 ± 0.020	4.21 ± 0.031	0.17 ± 0.003	1.23	0.79 ± 0.015
acetonitrile + H_2SO_4					1.59 ± 0.009	1.00			1.10	1.59 ± 0.009
acetonitrile + TEA					1.38 ± 0.517	0.12 ± 0.022	3.65 ± 0.071	0.88 ± 0.035	1.58	3.38 ± 0.158
dimethyl sulfoxide			7.03 ± 0.039	1.83	0.46 ± 0.010	0.84 ± 0.013	4.35 ± 0.057	0.16 ± 0.002	1.35	1.07 ± 0.016
methanol			4.45 ± 0.023	1.98	0.06 ± 0.006	0.85 ± 0.063	4.43 ± 0.037	0.15 ± 0.007	1.65	0.73 ± 0.032
tetrahydrofuran					0.63 ± 0.012	0.84 ± 0.009	4.81 ± 0.050	0.16 ± 0.002	1.15	1.29 ± 0.017
trifluoroethanol					0.41 ± 0.023	0.55 ± 0.009	1.84 ± 0.025	0.45 ± 0.013	1.12	1.25 ± 0.029
water (pH 7)	0.84 ± 0.006	0.88	0.18 ± 0.004	2.18	0.24 ± 0.009	0.78 ± 0.018	5.02 ± 0.043	0.22 ± 0.003	1.10	1.26 ± 0.020
deuterium oxide (pD 7)			0.46 ± 0.004	0.92	0.59 ± 0.025	0.76 ± 0.020	5.38 ± 0.099	0.24 ± 0.005	3.17	1.73 ± 0.042

observed from the absorption spectra, the magnitude in the pK_a change calculated for the excited state is less when calculated from the emission spectra. The lack of complete agreement between the pK_a^* calculated from the absorption and fluorescence spectra suggests that equilibrium between the acidic and basic species is not fully established within the fluorescence lifetime. Thus, the pK_a^*determined by this method is a weighted average of ground- and excited-state pK_a's.

Fluorescence Lifetimes. The fluorescence lifetimes of aniline, indoline, and I2CA in various solvents are reported in Table 3. The fluorescence decays of aniline and indoline in all solvent systems examined are best fit to a single exponential. The addition of a second decay component to the fits of indoline and aniline does not significantly improve the reduced χ^2 parameter, indicating that a single exponential adequately represents the fluorescence decays of aniline and indoline in all solvents examined. In most cases, two exponentials were necessary to characterize the fluorescence behavior of I2CA. The average fluorescence lifetime was calculated as the average of the two decay components weighted by their corresponding normalized amplitudes.

Indoline Fluorescence Decays. The fluorescence lifetime of indoline is 4.45 ns in methanol, 4.30 ns in acetonitrile, and 7.03 ns in DMSO (see Table 3). The fluorescence lifetimes of indoline in nonaqueous solvents are comparable to fluorescence lifetimes that have been observed for indole in nonaqueous solvents (e.g., 4.3 ns in methanol[48]). The quantum yield indicates a nonradiative decay rate on the order of 10^8 s^{-1} due to nonradiative decay channels such as intersystem crossing and internal conversion to the ground state. The relationship between the fluorescence lifetime of indoline and solvent parameters such as the dielectric constant, dipole moment, solvochromatic polarity (π^*),[49,50] reaction field factor [$F(\epsilon_0, n)$],[51] $E_t(30)$,[52] and proton donating and accepting propensity[53] was examined; however, no significant correlation was found.

A stark contrast arises in the fluorescence decays of indoline in aqueous solvents, where an additional nonradiative decay channel gives rise to much shorter lifetimes than in nonaqueous solvents as shown in Figure 8 and Table 3. The decay time of indoline is 180 ps in H_2O and 460 ps in D_2O. Correspondingly, the measured quantum yield is reduced by an order of magnitude in water relative to its value in acetonitrile (Table 1). Apparently, water introduces a unique quenching process leading to the fast decay of the excited state. Furthermore, the fluorescence lifetime of indoline in water is strongly temperature-dependent. The temperature dependence plotted in Figure 9 yields an activation energy of 7.9 kcal/mol with a frequency factor of 3.4×10^{15} s^{-1} (Table 4). These values are similar to values reported for indoles in water.[15,48,54]

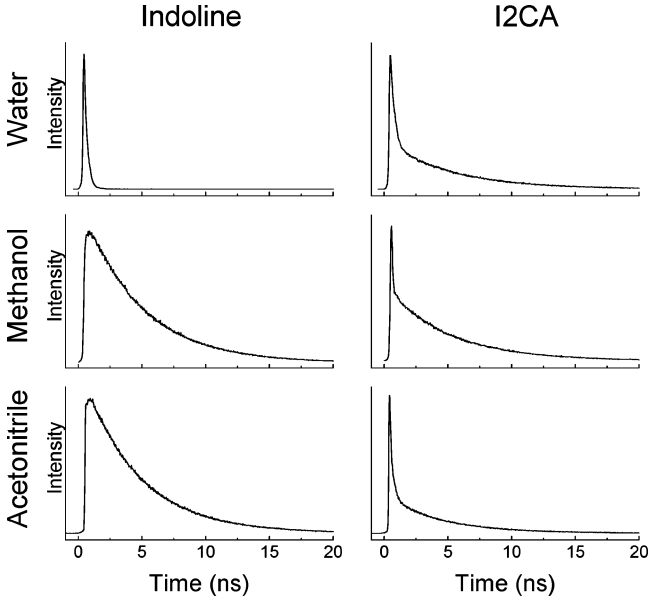

Figure 8. Fluorescence decays of indoline and I2CA in water (pH 7, top), methanol (middle), and acetonitrile (bottom).

Because the electronic states and electronic transitions of indoline closely resemble those in aniline,[25] it is instructive to compare the fluorescence decays of indoline to those of aniline in the same solvents. The fluorescence decays of aniline in

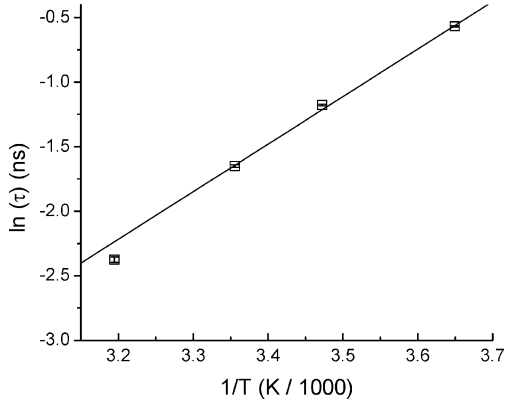

Figure 9. Arrhenius plot of the fluorescence lifetime of indoline in water at neutral pH. Solid line is the linear fit. Error bars are shown inside data points.

TABLE 4: Arrhenius Parameters for Indoline and I2CA

	E_a (kcal/mol)	A (s^{-1})
indoline	7.90 ± 0.38	$3.35 \times 10^{15} \pm 2.21 \times 10^{15}$
I2CA fast component	6.90 ± 0.15	$4.23 \times 10^{14} \pm 1.07 \times 10^{14}$
I2CA slow component	1.17 ± 0.12	$1.52 \times 10^{9} \pm 3.17 \times 10^{8}$

acetonitrile and in water follow a pattern similar to the decays in indoline. The aniline decays are single-exponential, with faster decay in water (0.84 ns) than in acetonitrile (2.9 ns; Table 3). Similar results have been reported previously for aniline.[55]

Several mechanisms of the deactivation of the excited state have been proposed for aromatic amines in aqueous solvents. These include proton transfer, electron transfer, and photoionization. Electron transfer to solvent could generate a solvated electron stabilized in a network of water molecules, or it could result in a charge-transfer exciplex.[48] Another possible decay channel could be introduced by the dissociation of a hydrogen bond to the amine group in the excited state due to the decrease in the pK_a of the amine in the excited state.

As with indoline, indoles also display a pronounced solvent dependence in the fluorescence lifetimes, with faster decay in aqueous solvents than in nonaqueous solvents.[12] Indole differs from indoline in the presence of a $C_2{=}C_3$ double bond and, spectroscopically, by overlapping ^1L_a and ^1L_b states in indole. The excited-state decays of indoline and aniline in H_2O and D_2O are significantly faster than the excited-state decay in indole in the same solvents. Nevertheless, the isotope effect in the fluorescence lifetime for indoline and aniline parallels that for indoles.[15,48,54,56] The magnitude of the isotope effect for indole, 1.54, agrees approximately with that for aniline.[55] For indoline, the isotope effect is larger (2.56, see Table 3) and the lifetimes are significantly shorter than for indole but comparable to those for aniline. It is our assertion that similar decay mechanisms operate in indoline, aniline, and indoles.

We measured the dependence of the fluorescence decay time for indoline on the mole fraction of water in water/methanol and water/acetonitrile mixtures. The dependence, shown in Figure 10, is similar to that observed for indole[14] and aniline.[55] As the fraction of water increases in mixed methanol/water solutions or mixed acetonitrile/water solutions, the fluorescence level at first remains constant or decreases slightly. Then, at mole fractions greater than 0.2 (acetonitrile/water) or 0.5 (methanol/water), the lifetime decreases more steeply. The nonlinear dependence, with a plateau at low mole fractions of water followed by a steeper dependence at higher mole fractions of water, suggests that the quenching mechanism requires a cluster of water molecules. Such behavior can be interpreted,

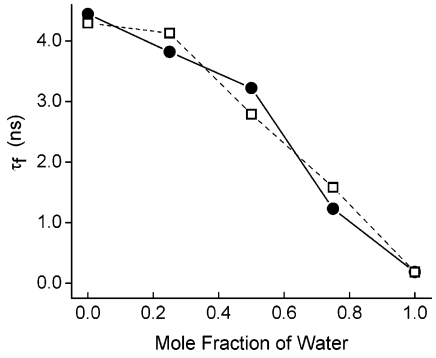

Figure 10. Average fluorescence lifetime of indoline as a function of the mole fraction of water. Water/methanol solutions (●) and water/acetonitrile solutions (□).

following Lee and Robinson, as electron transfer to a solvent cluster.[14] Alternatively, fluorescence quenching may be mediated by hydrogen bonding to a water cluster.[55] A third possibility is proton transfer to a solvent cluster. Each of these mechanisms may be accompanied by an isotope effect.

In a thorough consideration of potential quenching mechanisms in indoles, Barkley and co-workers concluded that the quenching of indoles in aqueous solvents occurs by electron transfer to a solvent O−H (or O−D) bond to form an exciplex.[54] This process in indoles is characterized by frequency factors that are 2- to 3-fold larger in H_2O than in D_2O.[54,56] On the basis of a study of excited-state decay rates in mixed aqueous and nonaqueous solvents, Lee and Robinson concluded that fluorescence quenching in indoles is facilitated by clusters of 4 ± 1 water molecules,[14] and they suggested that the underlying decay mechanism involves electron ejection to solvent. A similar finding was reported for aniline.[55] On the basis of the magnitude of the isotope effect and the Arrhenius frequency factor and activation energy, Barkley and co-workers have argued that the formation of a charge-transfer exciplex by electron transfer to an O−H (or O−D) bond is more likely to lead to the substantial isotope effect (2 to 3) observed in these systems,[55] as opposed to the photogeneration of a solvated electron. It is likely that the same mechanism is operative for indoline. This hypothesis is supported by the activation energy and frequency factor measured for indoline (Table 4). The high value of the frequency factor (3.4×10^{15} s^{-1}) argues strongly for an electron-transfer mechanism of fluorescence quenching in indoline as in indole. The fluorescence lifetime is constant from pH 5 to 10 (data not shown). This argues against proton transfer as a factor in the short lifetime over this pH range.

Indoline-2-Carboxylic Acid Fluorescence Decays. Table 3 presents fluorescence decay data for I2CA in several solvents. Fluorescence decays of I2CA in acetonitrile, methanol, and water are shown in Figure 8. The fluorescence decays of I2CA are more complex than those of indoline. In most solvents, the fluorescence decays are fit by double-exponential decays consisting of a fast subnanosecond component and a longer decay of 4 to 5 ns. This is in contrast to indoline itself, which exhibits a single time constant of 4 ns or longer in nonaqueous samples and a single subnanosecond time constant in aqueous solution. For I2CA in each of the nonaqueous solvents studied, a subnanosecond fluorescence decay component represents 75 to 85% of the decay amplitude. The remaining 15 to 25% of the amplitude decays in 4 to 5 ns (except in trifluoroethanol, where the decay time is 2 ns). Changes in this pattern were observed upon the addition of a small amount of acid (H_2SO_4) or base (triethylamine) to acetonitrile.

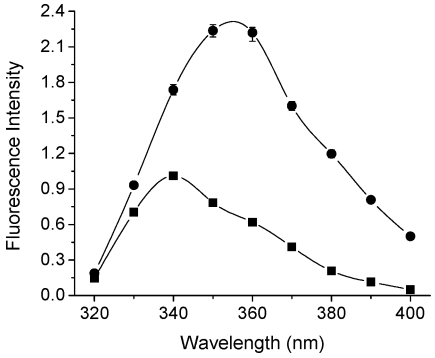

Figure 11. Decay-associated spectra of I2CA in acetonitrile at neutral pH. Fast-decay component (■) and the slow-decay component (●). Error bars are shown or fall inside the data points.

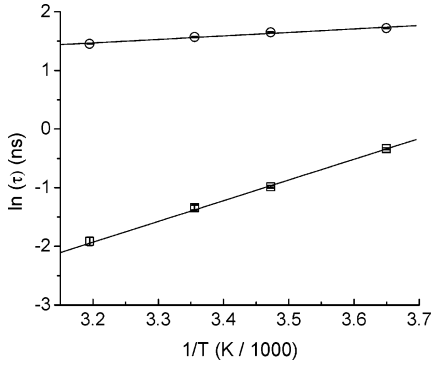

Figure 12. Arrhenius plot of the fast and slow components of the fluorescence lifetime of I2CA in water at neutral pH. Fast-decay component (□) and slow-decay component (○).

To elucidate the processes underlying these decay components, fluorescence decays of I2CA in acetonitrile were measured at a series of emission wavelengths from 320 to 400 nm and were used to obtain the decay-associated spectra shown in Figure 11. Two distinct fluorescence decay components were observed with essentially constant fluorescence lifetimes of 0.15 and 4.0 ns throughout the region. The amplitudes of the decay components were used to generate decay-associated spectra. The spectrum associated with the fast decay is peaked around 340 nm whereas the spectrum associated with the slow-decay component is peaked near 350 nm. The result is a shift of the emission spectrum toward the red during the fast-decay process.

The presence of two decay components might be explained by either of two very different mechanisms, one representing a static, ground-state process and the other, an excited-state process. In the ground-state process, two decay components result from two ground-state species that, upon excitation, decay with different fluorescence lifetimes. In the excited-state mechanism, the initially excited fluorescent species decays to another fluorescent species via an excited-state reaction such as proton transfer. An excited-state mechanism might be expected to manifest itself by a negative amplitude on the long-wavelength side of the fluorescence band, and such a component has not been observed. However, the absence of a detectable negative amplitude is not in itself sufficient to decide between the two mechanisms. It is likely, given the broad width of the emission associated with the fast decay and the small spectral shift, that a rise on the long-wavelength side of the emission band would not be detectable.

It is, however, possible to decide between a static, ground-state process and an excited-state reaction by comparing the measured and calculated fluorescence quantum yields (Table 1). The measured fluorescence quantum yield of I2CA in acetonitrile is approximately 0.03. With the reasonable assumption that the two ground-state species have the same radiative lifetime, the quantum yield of each species is given by its lifetime divided by the radiative lifetime, and the overall quantum yield is the sum of the quantum yield for each contributing species weighted by its fractional population. This yields the value of 0.03, which matches the measured value. In contrast, if the fast lifetime represented an excited-state reaction generating a second excited-state species that then fluoresced with the longer lifetime, then the measured quantum yield would be expected to match the value calculated as the ratio of the long lifetime to the radiative lifetime. This would lead to a quantum yield of up to 0.18.

Thus, the comparison of calculated and measured lifetimes indicates the presence of two ground-state species, one with a short fluorescence lifetime (163 ps) and one with a long lifetime (4.3 ns). A likely possibility is that these two conformations differ by the orientation of the carboxylic OH group with respect to the amine. Ab initio calculations and geometry optimizations (described in the companion paper[25]) indicate the presence of two conformations of I2CA, one with an intramolecular hydrogen bond between the carboxylic OH and the amine and one without this hydrogen bond. The hydrogen-bonded conformation is predicted to be lower in energy by 0.75 kcal/mol, suggesting that both species are present in solution with the intramolecularly hydrogen bonded species the more prevalent form.[25] These results suggest that the shorter fluorescence decay component corresponds to the hydrogen-bonded conformation. We propose that the presence of a hydrogen bond between the carboxylic OH and the amine N provides a fast deactivation channel that quenches the fluorescence by hydrogen bond dissociation. In the conformation lacking this hydrogen bond, this quenching is absent. The relative amplitudes suggest that the hydrogen-bonded conformation represents about 85% of the population in acetonitrile, DMSO, methanol, and tetrahydrofuran. The assignment of the fast-decay process to the intramolecularly hydrogen-bonded conformation is thus consistent with the ab initio calculations, which predict that this conformation is lower in energy. The amplitude of the fast component is lower (51%) in trifluoroethanol (TFE), which, as a stronger hydrogen bond donor than methanol, may decrease the population of intramolecularly hydrogen-bonded I2CA. The faster decay of the minor, long-lifetime component in TFE may result from excited-state proton transfer to the solvent.[56]

For I2CA in water, somewhat different considerations apply. At pH 7, I2CA exists as an anion. Ab initio calculations of the anion again show two possible conformations, one with a carboxylate oxygen in close proximity to the amine nitrogen, suggestive of a hydrogen bond, and the other without such an interaction.[25] The hydrogen-bonded species is predicted to be the more stable. The fluorescence decay again displays two components, one having a lifetime of 0.24 ns and the other, 5.0 ns. The close match between the measured quantum yield and the quantum yield calculated from the average fluorescence lifetime again indicates the presence of two species, one with a fast-decay time (0.24 ns in water) and the other with a long decay time (5.0 ns). An isotope effect of a factor of 2.5 is evident in the fast component from measurements in D_2O. The similarity of this value to the isotope effect of 2.6 that we found for indoline (Table 3) suggests that a similar quenching mechanism is operative (e.g., the formation of a charge-transfer exciplex).

An Arrhenius plot of the fast and slow lifetimes of I2CA is shown in Figure 12, and values are tabulated in Table 4. Temperature-dependent studies of the decay process in water yield an activation energy of 6.9 kcal/mol with a preexponential

factor of 4×10^{14} s^{-1}. In contrast, the frequency factor for indoline, like that for indoles,[15,54] is greater than 10^{15} s^{-1}. The value of the preexponential factor is significantly higher than the vibrational frequency of a hydrogen stretching vibration. The magnitude of the frequency factor and its similarity to values for indoles would seem to indicate a process that involves electron transfer, such as charge transfer to solvent to form an exciplex.

The slow component of the fluorescence decay of I2CA in water, representing 21% of the decay amplitude, decays by a different mechanism that is much less temperature-dependent with an activation energy of 1.2 kcal/mol. Ab initio calculations predict the presence of two conformations of the I2CA anion, differing in the orientation of the carboxylate group.[25] The fluorescence decay results suggest that one conformation is susceptible to decay by electron transfer to solvent, leading to the fast decay of the excited state, whereas the other conformation does not decay via an electron-transfer channel, leading to a long fluorescence lifetime.

Conclusions

We have studied the spectroscopic and photophysical properties of indoline and its 2-carboxylic acid derivative, I2CA. Unlike the related indoles, the ^1L_a and ^1L_b states of these compounds are well separated so that fluorescence originates unambiguously in the ^1L_b state. The amine group lends both compounds pH sensitivity with a pK_a of 4.7 to 5.3. Above this pH, however, the fluorescence properties of indoline and I2CA are not sensitive to pH, suggesting that the excited-state decay processes in aqueous solutions do not involve proton transfer. This makes I2CA an excellent fluorescence probe under physiological conditions. The fluorescence emission spectra and fluorescence lifetimes of both species are only moderately solvent-dependent in nonaqueous solvents. In contrast, the fluorescence lifetime of indoline, which is in the range of 4 to 7 ns in nonaqueous solvents, is much shorter in water, about 0.2 ns. The temperature dependence of this fast-decay process implicates an electron-transfer mechanism, and we propose that a mechanism similar to one proposed for indoles[12] is operative for indoline in water.

The spectroscopic and photophysical properties of the acid derivative, I2CA, are more complex for several reasons. First, the presence of the acid group leads to the mixing of ^1L_a and ^1L_b character in the two lowest lying transitions. This mixing has been characterized further by quantum calculations in the companion paper.[25] Second, quantum calculations show that two stable conformations differing in the orientation of the carboxylic acid group exist with nearly the same energy.[25] These two conformations appear to be responsible for the presence of two excited-state decay times in both nonaqueous and aqueous solvents. Finally, in aqueous solvents, the acid group introduces a second acid−base equilibrium with a pK_a of 3.3 for the carboxylic acid group. Consequently, at neutral pH, I2CA, like proline, exists as an anion.

In our laboratory, we have substituted I2CA as a fluorescent amino acid in short peptides.[26,28] The five-membered ring in I2CA forms the amino acid proline. Thus, I2CA can serve as a fluorescent proline analogue. Probing biomolecules by fluorescence often relies on the intrinsically fluorescent residues tyrosine, tryptophan, and phenylalanine. I2CA has a quantum yield that is similar to that of tryptophan, and its fluorescence lifetime is amenable to fluorescence studies of small biomolecules. In fluorescence depolarization studies of the orientational dynamics of peptides, the localized motion of the side chains of the native fluorescent amino acids often dominates the anisotropy decay. The incorporation of indoline into the peptide backbone allows the dynamics of the peptide backbone to be probed directly.

Acknowledgment. We thank Paul Hanson, Andrew Borovik, and Cynthia Larive for the gift of solvents and assistance with purification. B.D.S. and J.R.U. acknowledge support from a training grant in Dynamic Aspects of Chemical Biology (NIH 5 T32 GM08545-09). Acknowledgment is made to the donors of the Petroleum Research Fund, administered by the American Chemical Society, for supporting this research.

References and Notes

(1) Beechem, J. M.; Brand, L. *Annu. Rev. Biochem.* **1985**, *54*, 43.
(2) Chen, Y.; Barkley, M. D. *Biochemistry* **1998**, *37*, 9976.
(3) Petrich, J. W.; Chang, M. C.; Fleming, G. R. *NATO ASI Ser., Ser. A* **1985**, *85*, 77.
(4) Callis, P. R. *Methods Enzymol.* **1997**, *278*, 113.
(5) Rayner, D. M.; Szabo, A. G. *Can. J. Chem.* **1978**, *56*, 743.
(6) Szabo, A. G.; Rayner, D. M. *J. Am. Chem. Soc.* **1980**, *102*, 554.
(7) Robbins, R. J.; Fleming, G. R.; Beddard, G. S.; Robinson, G. W.; Thistlethwaite, P. J.; Woolfe, G. J. *J. Am. Chem. Soc.* **1980**, *102*, 6271.
(8) Petrich, J. W.; Chang, M. C.; McDonald, D. B.; Fleming, G. R. *J. Am. Chem. Soc.* **1983**, *105*, 3824.
(9) Chen, Y.; Liu, B.; Yu, H.-T.; Barkley, M. D. *J. Am. Chem. Soc.* **1996**, *118*, 9271.
(10) Bent, D. V.; Hayon, E. *J. Am. Chem. Soc.* **1975**, *97*, 2612.
(11) Bryant, F. D.; Santus, R.; Grossweiner, L. I. *J. Phys. Chem.* **1975**, *79*, 2711.
(12) Yu, H. T.; Colucci, W. J.; McLaughlin, M. L.; Barkley, M. D. *J. Am. Chem. Soc.* **1992**, *114*, 8449.
(13) Chang, M. C.; Petrich, J. W.; McDonald, D. B.; Fleming, G. R. *J. Am. Chem. Soc.* **1983**, *105*, 3819.
(14) Lee, J.; Robinson, G. W. *J. Chem. Phys.* **1984**, *81*, 1203.
(15) Lee, J.; Robinson, G. W. *J. Phys. Chem.* **1985**, *89*, 1872.
(16) Donzel, B.; Gaudchon, P.; Wahl, P. *J. Am. Chem. Soc.* **1974**, *96*, 801.
(17) Colucci, W. J.; Tilstra, L.; Sattler, M. C.; Fronczek, F. R.; Barkley, M. D. *J. Am. Chem. Soc.* **1990**, *112*, 9182.
(18) Tilstra, L.; Sattler, M. C.; Cherry, W. R.; Barkley, M. D. *J. Am. Chem. Soc.* **1990**, *112*, 9176.
(19) McMahon, L. P.; Yu, H.-T.; Vela, M. A.; Morales, G. A.; Shui, L.; Fronczek, F. R.; McLaughlin, M. L.; Barkley, M. D. *J. Phys. Chem. B* **1997**, *101*, 3269.
(20) Callis, P. R. *Methods Enzymol.* **1997**, *278*, 113.
(21) Callis, P. R. *J. Chem. Phys.* **1991**, *95*, 4230.
(22) Eftink, M. R.; Selvidge, L. A.; Callis, P. R.; Rehms, A. A. *Proc. SPIE-Int. Soc. Opt. Eng.* **1990**, *1204*, 171.
(23) Slater, L. S.; Callis, P. R. *J. Phys. Chem.* **1995**, *99*, 8572.
(24) Sun, M.; Song, P.-S. *Photochem. Photobiol.* **1977**, *25*, 3.
(25) Slaughter, B. D.; Lushington, G. H.; Allen, M. W.; Johnson, C. K. *J. Phys. Chem. A* **2003**, *107*, 5670.
(26) Bothwell, T.; Allen, M. W.; Hedstrom, J. F.; Johnson, C. K. *J. Phys. Chem. B*, submitted for publication, 2003.
(27) Johnson, C. K.; Bothwell, T. G.; Allen, M. W.; Osborn, K. D. *Biophys. J.* **2001**, *80*, 360a.
(28) Allen, M. W.; Bothwell, T. G.; Slaughter, B. D.; Johnson, C. K. *Biophys. J.* **2002**, *82*, 428a.
(29) Allen, M. W.; Slaughter, B. D.; Larive, C. K.; Johnson, C. K. Unpublished data.
(30) Harms, G. S.; Pauls, S. W.; Hedstrom, J. F.; Johnson, C. K. *J. Fluoresc.* **1997**, *7*, 273.
(31) Beechem, J. M.; Gratton, E. *Proc. SPIE-Int. Soc. Opt. Eng.* **1988**, *909*, 70.
(32) Lakowicz, J. R. *Principles of Fluorescence Spectroscopy*, 2nd ed.; Kluwer Academic/Plenum Publishers: New York, 1983.
(33) Chen, R. F. *Anal. Lett.* **1967**, *1*, 35.
(34) Strickler, S. J.; Berg, R. A. *J. Chem. Phys.* **1962**, *37*, 814.
(35) Birks, J. B.; Dyson, D. J. *Proc. R. Soc. London, Ser. A* **1963**, *275*, 135.
(36) Schiebener, P.; Straub, J.; Sengers, J. M. H. L.; Gallagher, J. S. *J. Phys. Chem. Ref. Data* **1990**, *19*, 677.
(37) Petruska, J. *J. Chem. Phys.* **1961**, *34*, 1120.
(38) Kassab, E.; Evleth, E. M. *Understanding Chem. React.* **1999**, *20*, 231 (Role of Rydberg States in Spectroscopy and Photochemistry).
(39) Bridges, J. W.; Williams, R. T. *Biochem. J.* **1968**, *107*, 225.
(40) Albert, A.; Serjeant, E. P. *Ionization Constants of Acids and Bases*; Wiley & Sons: New York, 1962.

(41) Brown, H. C.; McDaniel, D. H.; Hafliger, O. Dissociation Constants. In *Determination of Organic Structures by Physical Methods*; Braude, E. A., Nachod, F. C., Eds.; Academic Press: New York, 1955; p 567.
(42) Förster, T. *Z. Elektrochem.* **1950**, *54*, 531.
(43) Weller, A. *Z. Elektrochem.* **1952**, *56*, 662.
(44) Bridges, J. W.; Davies, D. S.; Williams, R. T. *Biochem. J.* **1966**, *98*, 451.
(45) Grabowski, Z. R.; Rubaszewska, W. *J. Chem. Soc., Faraday Trans. 1* **1977**, *73*, 11.
(46) Lahiri, S. C. *J. Sci. Ind. Res.* **1979**, *38*, 492.
(47) Vander Donckt, E.; Porter, G. *Trans. Faraday Soc.* **1968**, *64*, 3215.
(48) Walker, M. S.; Bednar, T. W.; Lumry, R.; Humphries, F. *Photochem. Photobiol.* **1971**, *14*, 147.
(49) Laurence, C.; Nicolet, P.; Dalati, M. T.; Abboud, J.-L. M.; Notario, R. *J. Phys. Chem.* **1994**, *98*, 5807.
(50) Kamlet, M. J.; Abboud, J. L. M.; Abraham, M. H.; Taft, R. W. *J. Org. Chem.* **1983**, *48*, 2877.
(51) Reynolds, L.; Gardecki, J. A.; Frankland, S. J. V.; Horng, M. L.; Maroncelli, M. *J. Phys. Chem.* **1996**, *100*, 10337.
(52) Reichardt, C. *Chem. Rev.* **1994**, *94*, 2319.
(53) Reichardt, C. *Solvents and Solvent Effects in Organic Chemistry*, 2nd ed.; VCH: Weinheim, Germany, 1988.
(54) McMahon, L. P.; Colucci, W. J.; McLaughlin, M. L.; Barkley, M. D. *J. Am. Chem. Soc.* **1992**, *114*, 8442.
(55) Tobita, S.; Ida, K.; Shiobara, S. *Res. Chem. Intermed.* **2001**, *27*, 205.
(56) Chen, Y.; Liu, B.; Barkley, M. D. *J. Am. Chem. Soc.* **1995**, *117*, 5608.
(57) Mulliken, R. S.; Rieke, C. A. *Phys. Soc. Rep. Prog. Phys.* **1941**, *8*, 231.
(58) Birks, J. B. *Photophysics of Aromatic Molecules*. Wiley Monographs in Chemical Physics; Wiley & Sons: New York, 1970.